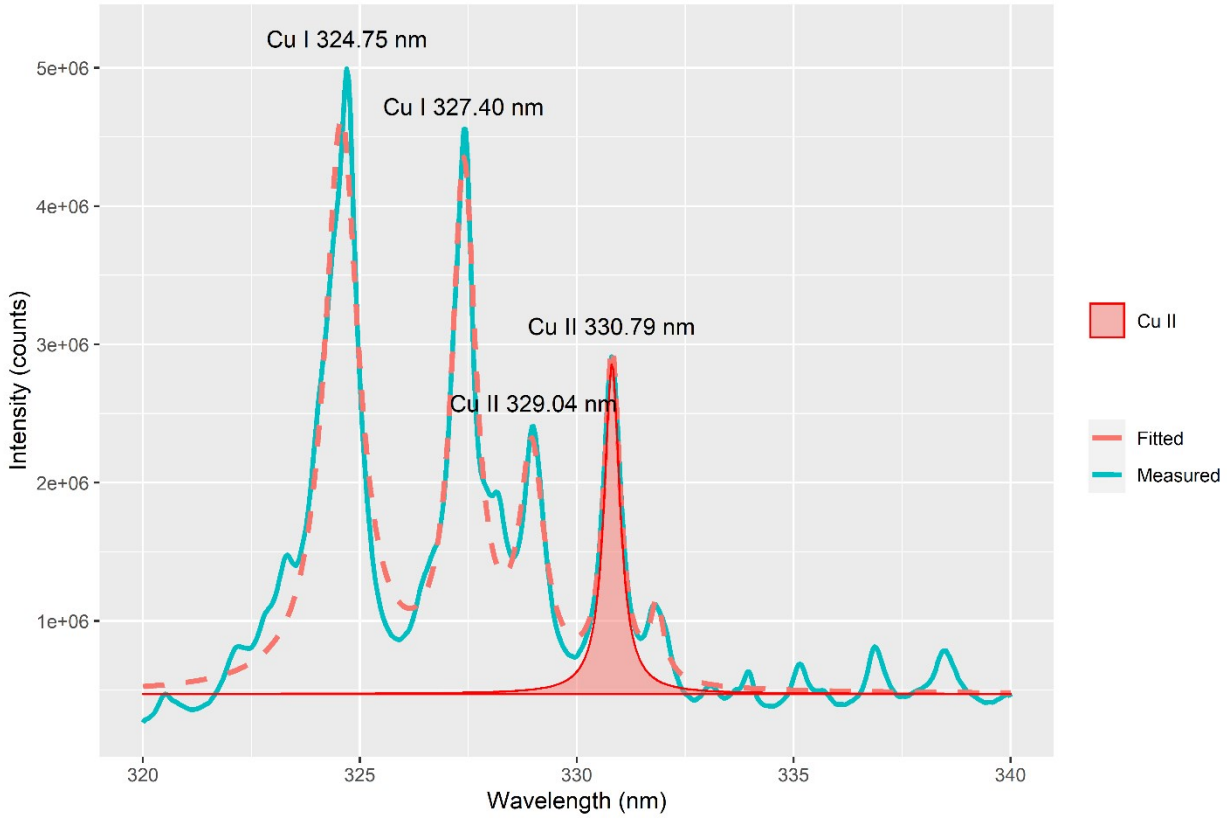

Figure S1. Recorded spectrum at $t_d = 1000$ ns with an 80 mJ ablation pulse energy at orthogonal pulse incidence. The shaded area was considered as the emission line intensity. Each major emission line was fitted by a Lorentzian profile.

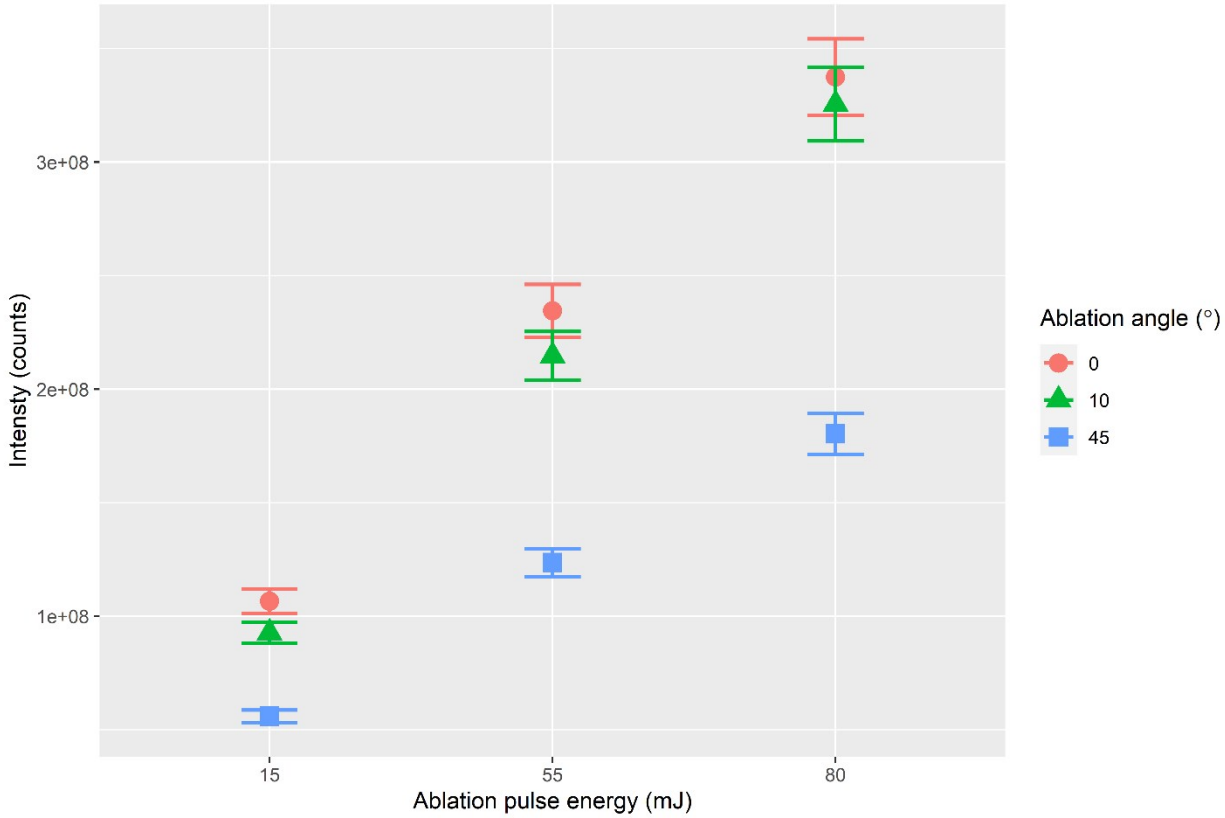

Figure S2. Intensity of the Cu I 521 nm emission line as a function of the ablation pulse energy for the explored ablation angles integrated over 5000 ns, starting at $t_d = 10$ ns after the ablation pulse.

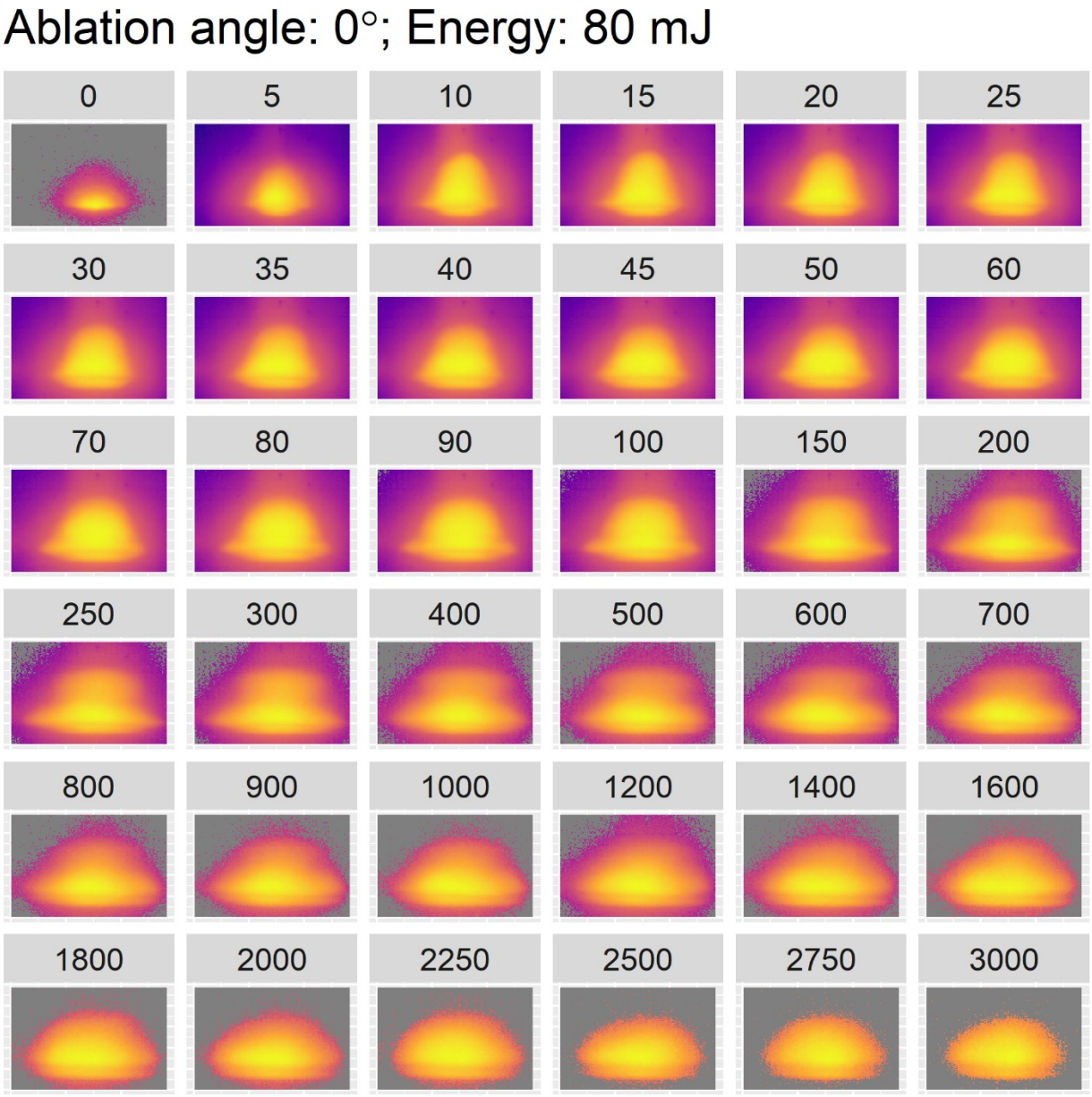

Figure S3. White-light images plasmas induced by orthogonal incidence angle at various delays after ablation (ns). The ablation energy was 80 mJ. The exposure time was 5 ns. The images were individually normalized to the 0–1 range.

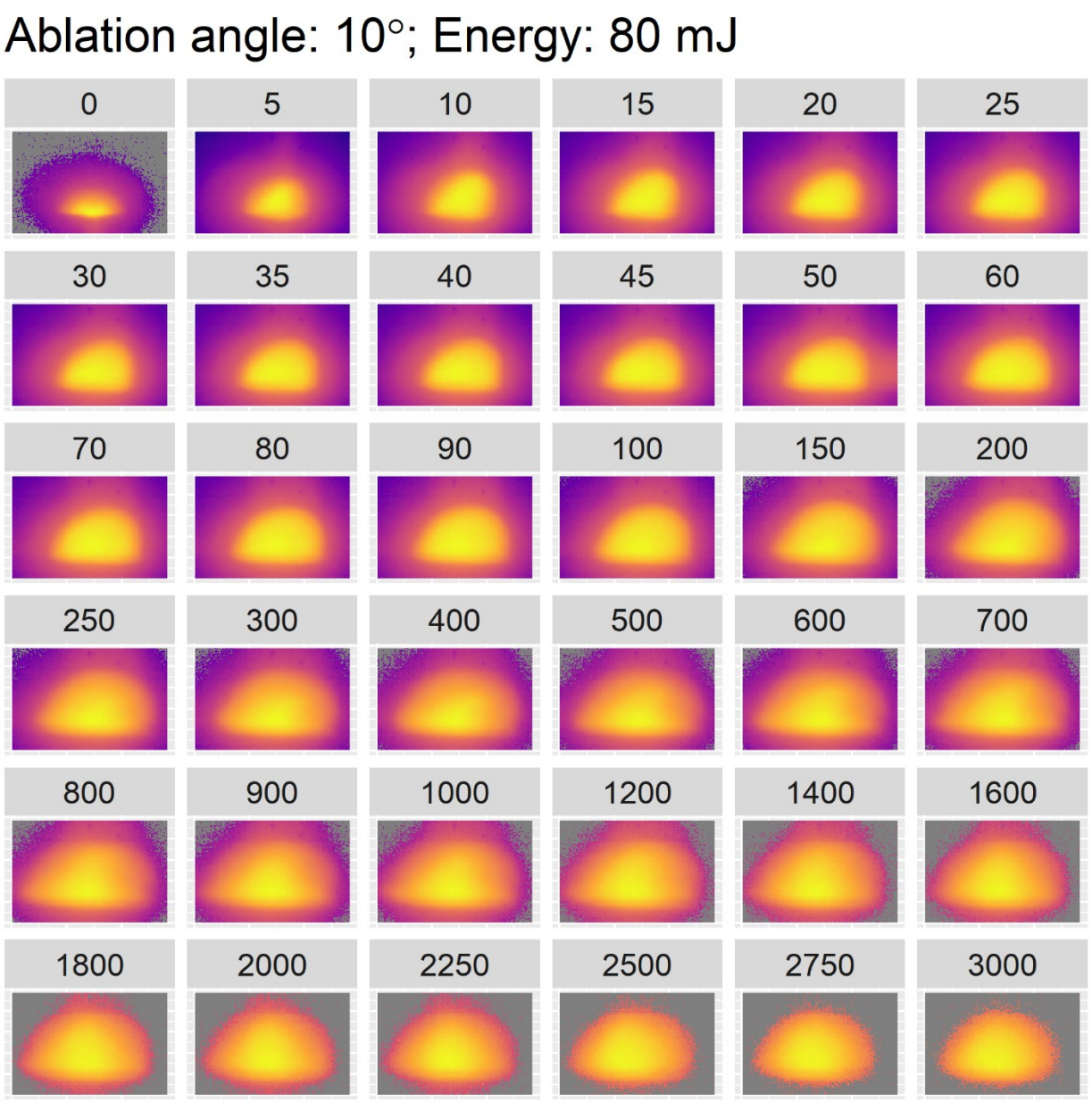

Figure S4. White-light images plasmas induced under a 10° incidence angle (measured from the sample normal) at various delays after ablation (ns). The ablation energy was 80 mJ. The exposure time was 5 ns. The images were individually normalized to the 0–1 range.

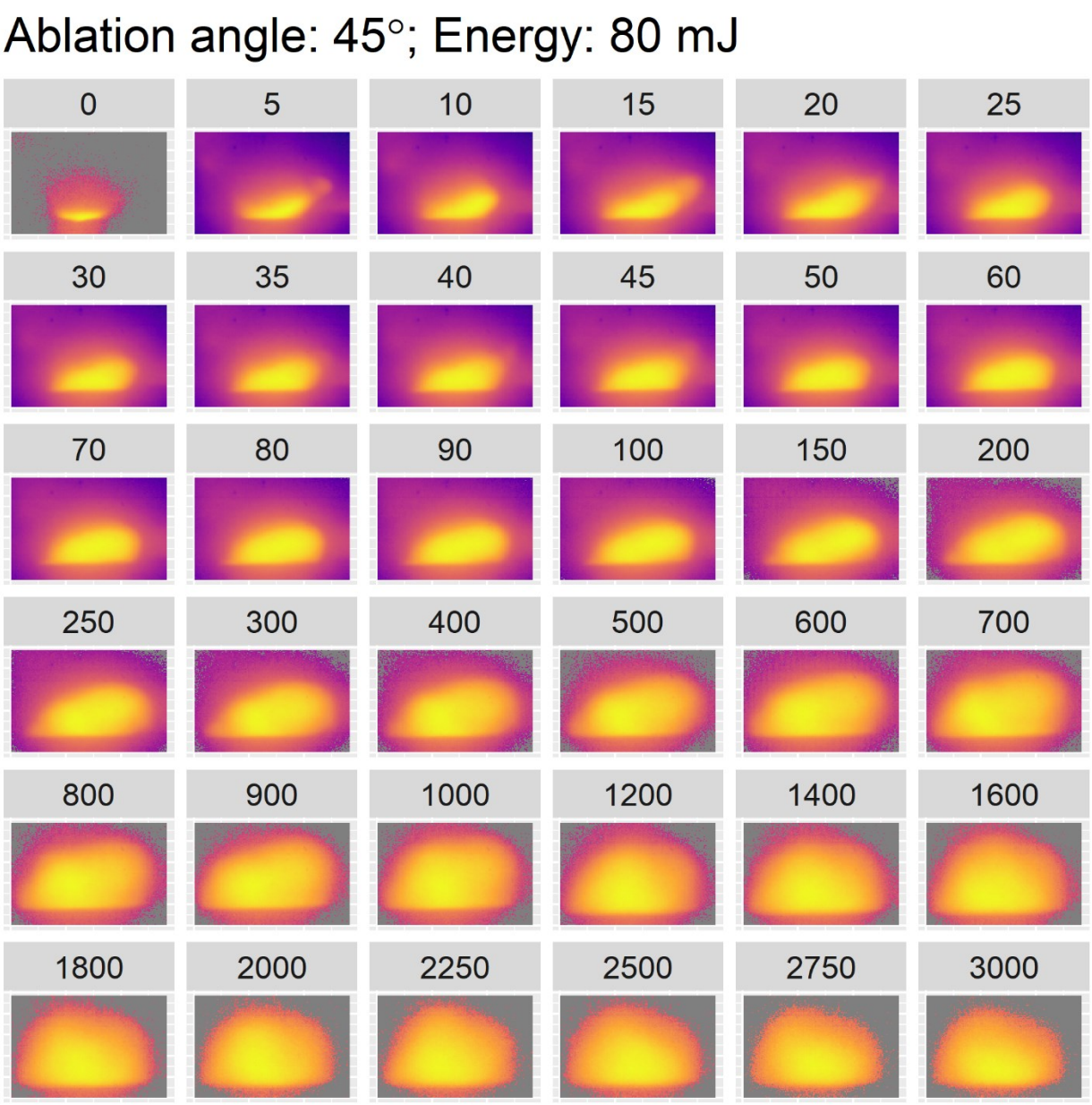

Figure S5. White-light images plasmas induced under a 45° incidence angle (measured from the sample normal) at various delays after ablation (ns). The ablation energy was 80 mJ. The exposure time was 5 ns. The images were individually normalized to the 0–1 range.

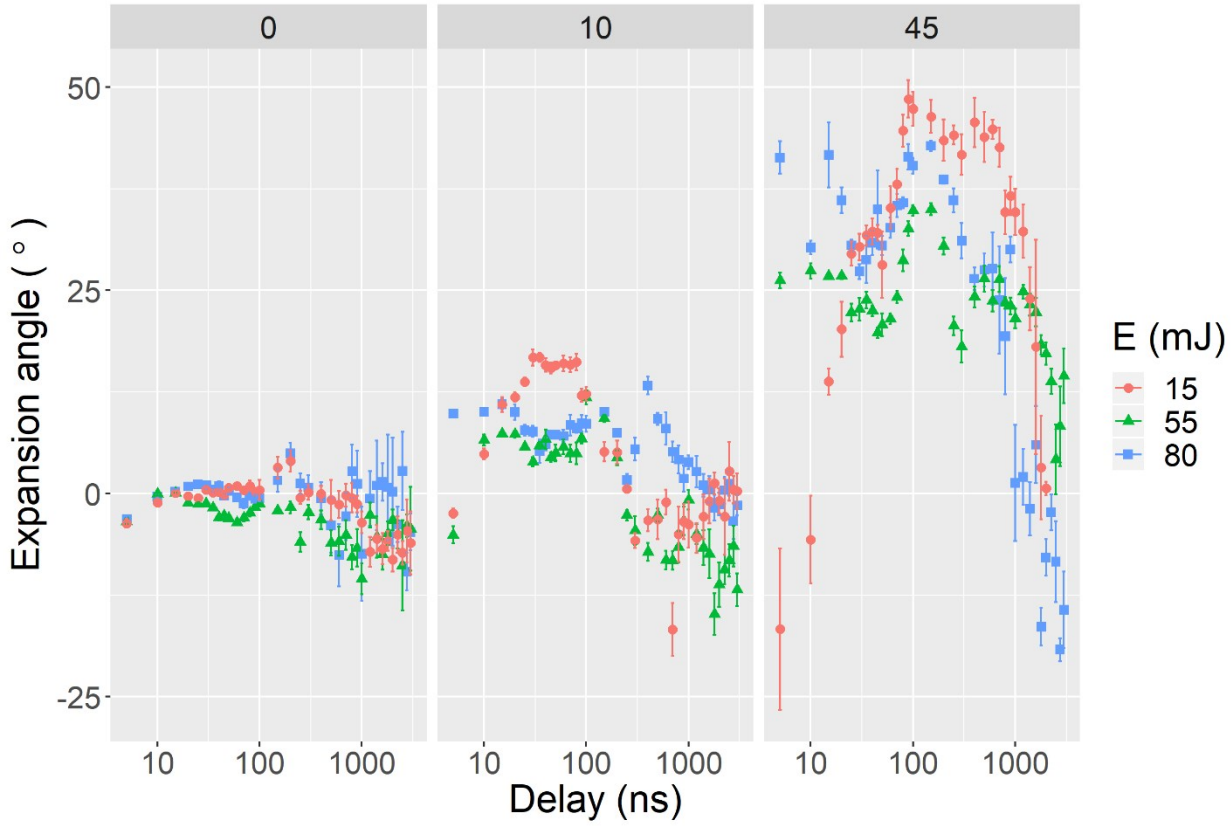

Figure S6. Apparent expansion angle of the plasma as function of time (logarithmic scale).

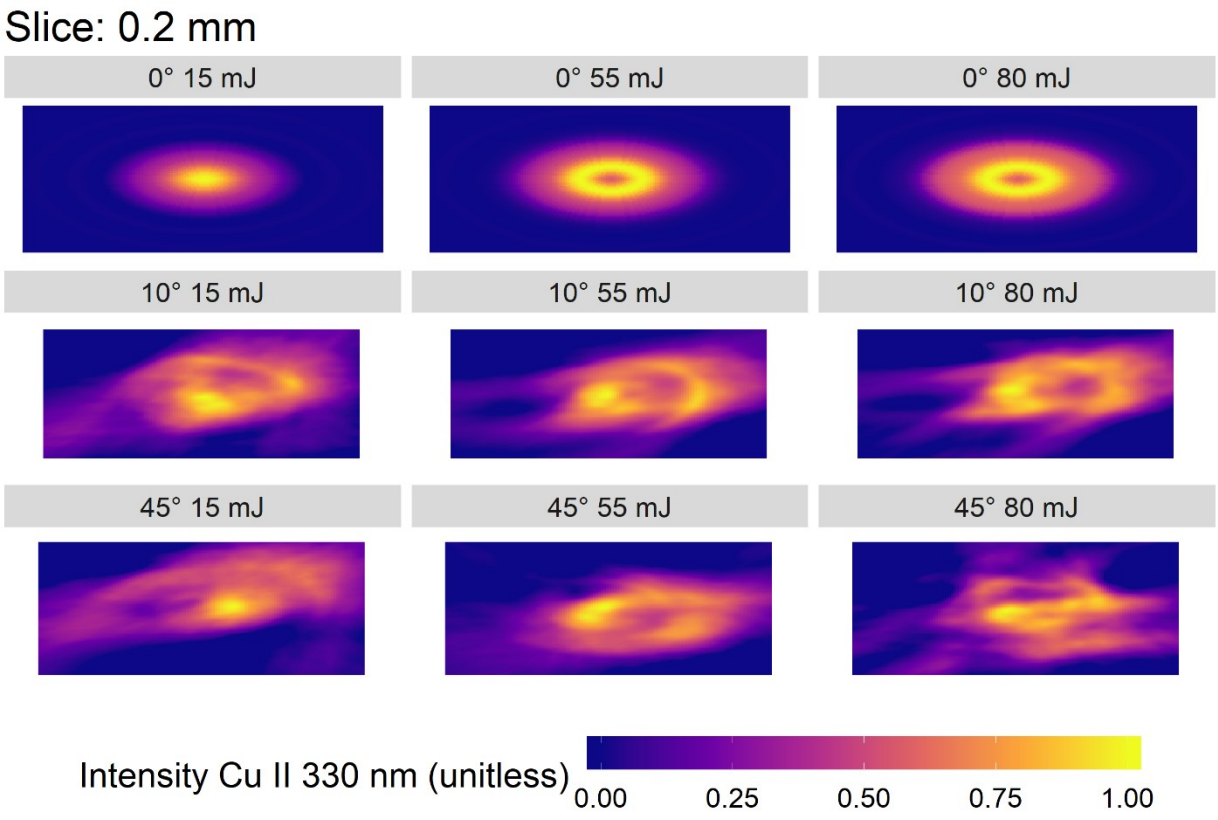

Figure S7. Reconstructed Cu II 330 nm emissivity in the horizontal plane 0.2 mm above the sample surface for plasmas induced with various ablation energies and incidence angles 300 ns after ablation. The emissivity distributions have been individually normalized to the 0—1 range.

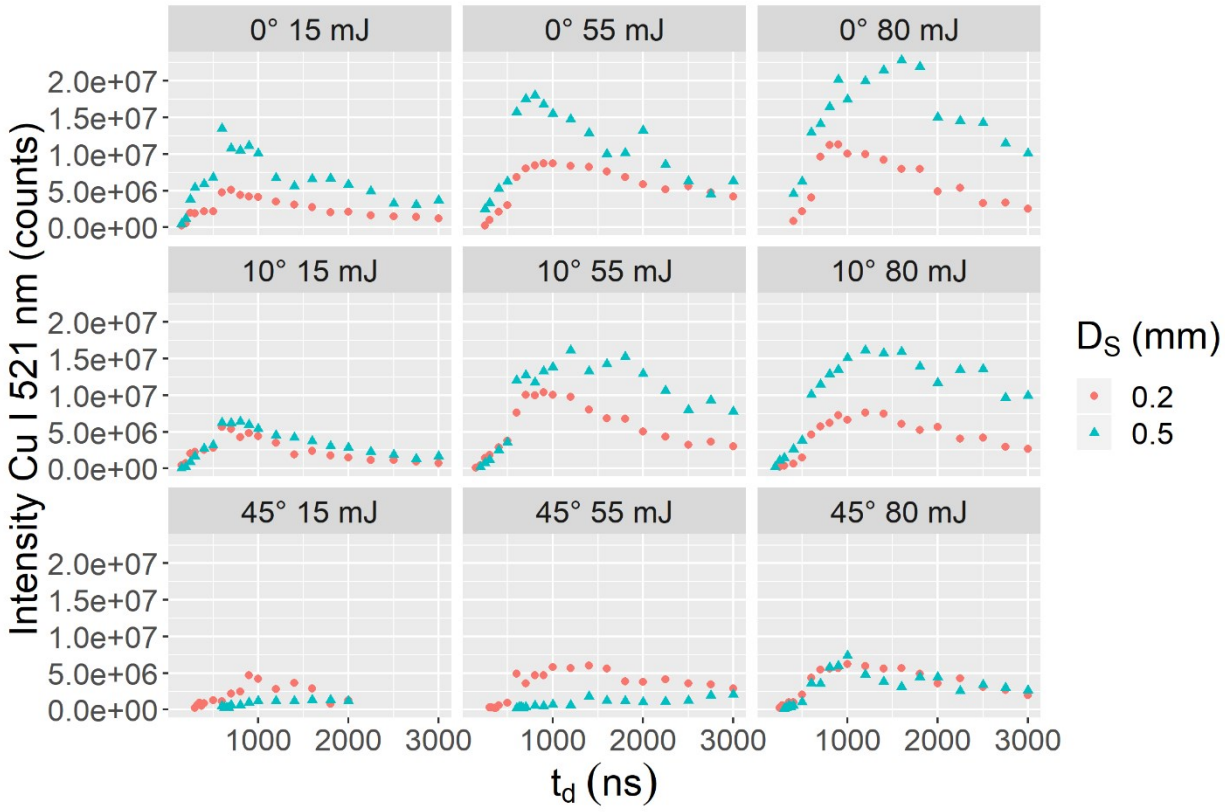

Figure S8. Atomic emission intensity (Cu I 521 nm) of the plasmas as function of time at two distinct heights above the sample surface for all three incidence angles and ablation energies. The estimated error of the values is 15 %.

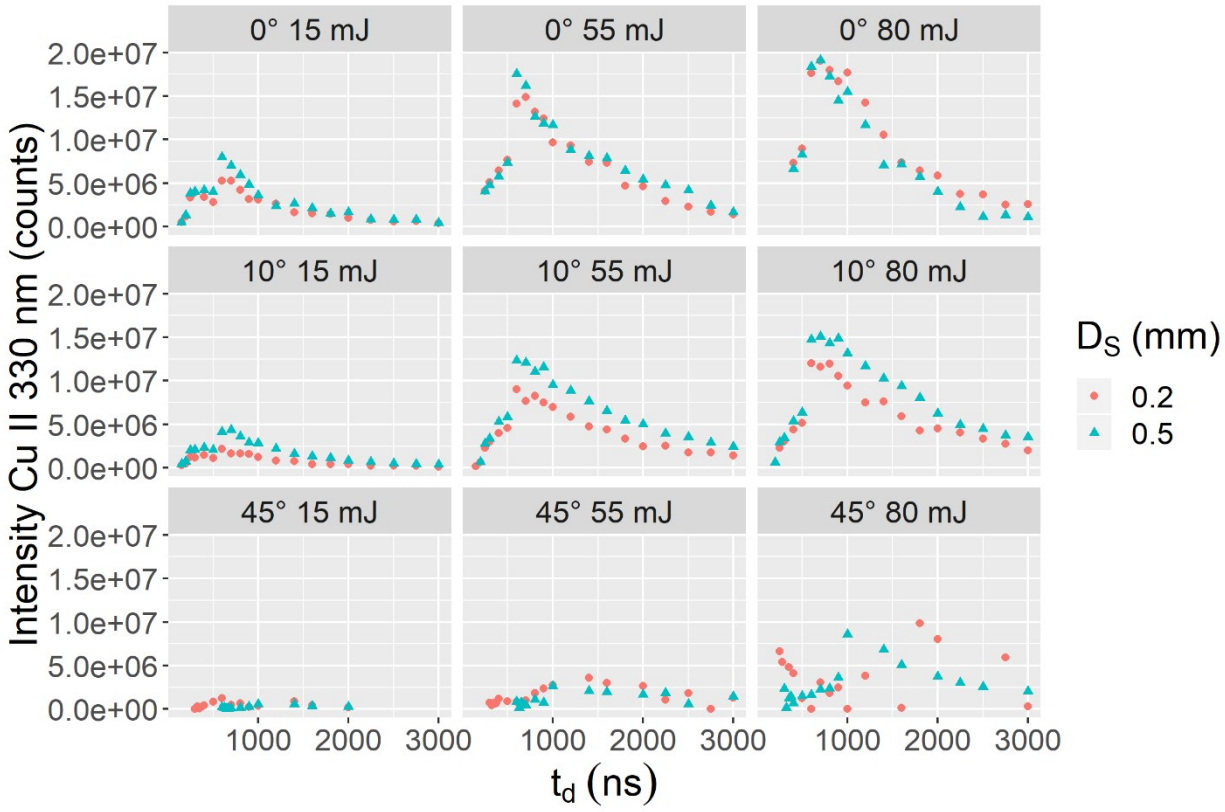

Figure S9. Ionic emission intensity (Cu II 330 nm) of the plasmas as function of time at two distinct heights above the sample surface for all three incidence angles and ablation energies. The estimated error of the values is 15 %.

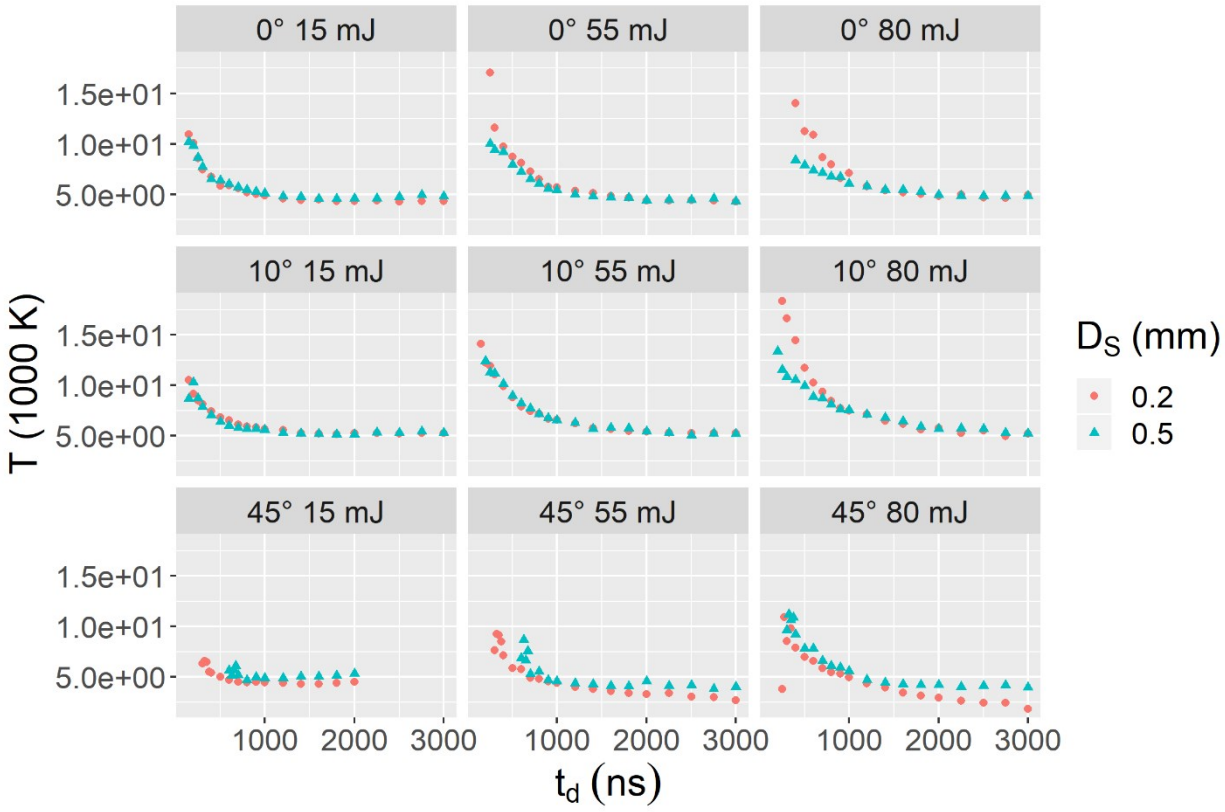

Figure S10. Electron temperature of the plasmas as function of time at two distinct heights above the sample surface for all three incidence angles and ablation energies. The estimated error of the values is 15 %.

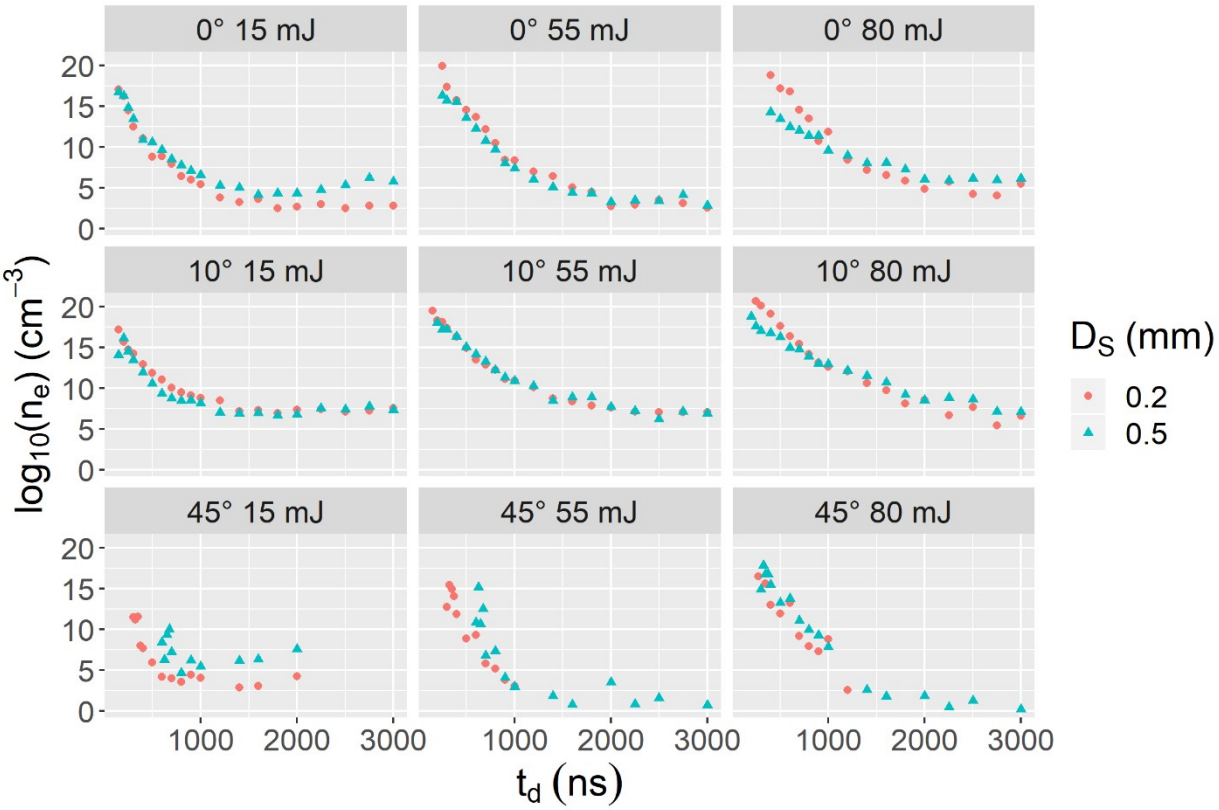

Figure S11. Electron density of the plasmas as function of time at two distinct heights above the sample surface for all three incidence angles and ablation energies. The estimated error of the values is 15 %.